RSC Advances

ROYAL SOCIETY OF CHEMISTRY

www.rsc.org/advances

Journal Name

ARTICLE

A Novel Heterobimetallic Ru(II)-Gd(III) Complex-Based Magnetoluminescent Agent for MR and Luminescence Imaging

Received 00th January 20xx,
Accepted 00th January 20xx

DOI: 10.1039/x0xx00000x

www.rsc.org/

Wenbo Shi,[a] Bo Song,[a] Mingqian Tan,[b] Zhiqiang Ye,*[a] and Jingli Yuan[a]

A novel heterobimetallic ruthenium(II)-gadolinium(III) complex, **Ru-Gd,** comprising a luminescent Ru(II) complex $[Ru(bpy)_2(phen)]^{2+}$ (bpy: 2,2'-bipyridine; phen: 1,10-phenanthroline), and a Gd(III) complex, DOTA-Gd^{3+} (DOTA: 1,4,7,10-tetraazacyclododecane-1,4,7,10-tetraacetic acid), has been designed and synthesized as a magnetoluminescent dual-modal imaging agent. The heterobimetallic complex **Ru-Gd** is water-soluble, biocompatible with low cytotoxicity, strongly luminescent with a long luminescence lifetime and a large Stokes shift, and has comparable longitudinal relaxativity r_1 (4.71 mM^{-1} s^{-1}), which enable the complex to be suitable for luminescence bioimaging and T_1-weighted MR imaging. Using **Ru-Gd** as a contrast agent, the T_1-weighted MRI of Kunming (KM) mouse was successfully carried out. The results demonstrated the availability and validity of our approach for the development of magnetoluminescent dual-modal imaging agents.

1. Introduction

In biological terms, the most straightforward way to get information is through our eyes. Therefore, biological imaging techniques, such as X-ray imaging, magnetic resonance imaging, bio-optical imaging and radio nuclide imaging, have attracted much attention of researchers.[1] Among these techniques, luminescence imaging and magnetic resonance imaging (MRI) have become increasingly popular in experimental molecular imaging and clinical diagnosis in recent years.[2,3] Luminescence imaging has achieved significant development in simplicity, specificity, and sensitivity both for in vivo and in vitro bioassays,[4] and also becomes a powerful tool for observing the morphology, structure and activity of cells.[5] However, luminescence imaging has the disadvantage that it cannot image thick tissue samples owing to the lack of its optical transparency.[6,7] In the past few decades, MRI technique has become an ideal method for providing whole body images[8] due to its strong function without damage to organisms.[9] However, MRI is also plagued by two shortcomings, poor spatial resolution in millimeter range[8] and low sensitivity.[10] In view of these limitations, the idea using multiple modalities in conjunction has gained in popularity, and researchers have recently sought to combine the three-dimensional and *in vivo* aspects of MRI with luminescence imaging technique in tandem, which is complementary in terms of both spatial resolution and imaging sensitivity.[11,12] This dual-modal imaging has the exciting potentials, for example, it can be used in diagnosis to track and identify tumor cells (via MRI) and in surgery to provide surgical guidance for the tumor resection in real time (via luminescence imaging).[13]

First of all, it requires the development of dual-modal imaging agents that could act as both MRI contrast agents and luminescent probes, so-called magnetoluminescent imaging agents. Ideally, dual-modal imaging agents integrate a reporter optimized for each of the imaging techniques within a nanomaterial or a small molecular entity. In recent years a number of magnetoluminescent imaging agents with particular interest in, for example, the utilisation of gadolinium chelates,[14] functionalised quantum dots[15] and iron oxide nanoparticles,[16,17] have been reported. The unique magnetic properties of gadolinium(III) ion are instrumental in enhancing the relaxation rate of water protons in tissues.[18-20] The stable Gd^{3+} complexes can reduce the toxicity of free Gd^{3+} ions[21] and enhance the T_1 (spin–lattice) and T_2 (spin–spin) relaxation rates of water protons in the proximity of the paramagnetic centre, Gd^{3+}. There are a range of commercially available Gd^{3+} complexes, such as ProHance and Gadovist,[22] which are routinely used in the clinical MRI diagnosis. The starting point for the development of magnetoluminescent imaging agents involves the conjugation of a Gd^{3+} complex with an organic fluorophore, such as fluorescein[23], tetramethylrhodamine-5-isothiocyanate (TRITC)[24] and cyanine dyes.[25] The use of organic dyes, however, is somewhat unsuitable for real-time imaging due to the rapid photobleaching of these dyes under the intense excitation light. As a promising alternative, luminescent transition metal complexes, especially those

[a] State Key Laboratory of Fine Chemicals, Department of Chemistry, Dalian University of Technology, Dalian 116024, China. Tel./Fax: +86-411-84986042; E-mail: yezq@dlut.edu.cn.
[b] Liaoning Key Laboratory of Food Biological Technology, School of Food Science and Technology, Dalian Polytechnic University, Dalian 116034, China.

†Electronic Supplementary Information (ESI) available: Luminescence spectra, decay traces of the Ru(II) complexes, and the supplementary Figures. See DOI: 10.1039/x0xx00000x

Ru(II), Re(I) and Ir(III), have attracted particular interest due to theirs desirable features including the intense visible excitation and emission, large Stokes shift, and high photo-, thermal and chemical stabilities.[26] Different from conventional fluorescent materials which are singlet state emitters, the luminescent transition metal complexes are triplet emitters having long emission lifetimes (>100 ns), which enables these complexes to be applied for the time-resolved luminescence imaging.[26] Furthermore, in comparison with nanoparticulate agents, small molecular magnetoluminescent imaging agents can avoid the toxicity that associated with long-term liver retention, and have the potential for more rapid diffusion through tissues.[21] Recently, a Gd-diethylenetriaminepentaacetic acid (DTPA) containing Ru (II) complex has been reported as a potential bimodal bioimaging agent.[27] However, the stability of the Gd-DTPA moiety would be affected by pH of the environment, while the DOTA-Gd moiety is stable in a wider pH range due to the complexation features of cryptands and the formation of a Gd inclusion complex. Based on the conjugation of a Re(I) complex with a Gd^{3+} complex, Koullourou and co-workers have synthesized a dual-model imaging agent,[28] and proved that the complex may be useful for luminescence imaging and MRI. However, its application for living cells and bodies has not been demonstrated.

Here we report the design and synthesis of a novel small molecular magnetoluminescent imaging agent, **Ru-Gd**, by conjugating a Ru(II) complex with a DOTA-Gd^{3+} complex. The agent is water-soluble, biocompatible, and has the long luminescence lifetime, high photo-, thermal and chemical stabilities and comparable longitudinal relaxativity r_1. The application of **Ru-Gd** in luminescence imaging experiments for live cells and in vivo MRI experiments for KM mouse proved that the novel agent is a useful dual-modal agent for luminescence and MR imaging.

2. Experimental

2.1 Materials and instruments

Human liver carcinoma cells (HepG2 cells) were obtained from the Dalian Medical University. The PBS buffer consisting of 137 mM NaCl, 2.7 mM KCl, 10.1 mM Na_2HPO_4 and 1.8 mM KH_2PO_4 was prepared in our laboratory. $[Ru(bpy)_2(phen\text{-}Br)](PF_6)_2$ and 1,4,7-tetraazacyclododecane-1,4,7-triacetic acid (DO3A) *tert*-butyl ester hydrobromide were synthesized according to the previously reported methods.[29-31] The reagent 3-(4,5-dimethyl-2-thiazoyl)-2,5-diphenyltetrazolium bromide (MTT) was purchased from Sigma-Aldrich. The solvents DMF and CH_3CN were used after appropriate distillation and purification. Unless otherwise stated, all chemical materials were purchased from commercial sources and used without further purification.

^1H and ^{13}C NMR spectra were measured on a Bruker Avance spectrometer (400 MHz for ^1H and 100 MHz for ^{13}C). Mass spectra were recorded on a HP1100 LC/MSD MS spectrometer. Elemental analysis was carried out on a Vario-EL analyser. Absorption spectra were measured on a Perkin-Elmer Lambda 35 UV-vis spectrometer. Emission lifetimes were measured on a FLS 920 steady/transient fluorescence spectrometer (Edinburgh Instruments). Luminescence spectra were measured on a Perkin-Elmer LS 50B luminescence spectrometer with excitation and emission slits of 10 nm. All bright-field and luminescence imaging measurements were carried out on a Nikon TE 2000-E luminescence microscope. The microscope, equipped with a 100 W mercury lamp, a Nikon B-2A filters (excitation filter, 450-490 nm; dichroic mirror, 505 nm; emission filter, > 590 nm) and a color CCD camera system (RET-2000R-F-CLR-12-C, Qimaging Ltd.), was used for luminescence imaging measurements with an exposure time of 3 s. The relative luminescence intensities of images were analyzed by using ImageJ software. The longitudinal and transverse relaxation times of water solutions with different concentrations of **Ru-Gd** were measured on a 0.5T NM12 magnetic resonance analyzer. The MRI measurements were carried out on a NMI20-030H-I Magnetic resonance imager from NIUMAG technology.

2.2 Synthesis of complex 1

A mixture of $[Ru(bpy)_2(phen\text{-}Br)](PF_6)_2$ (204 mg, 0.2 mmol), DO3A *tert*-butyl ester hydrobromide (514 mg, 1.0 mmol), and cesium carbonate (392 mg, 1.2 mmol) in 20 mL anhydrous acetonitrile was refluxed overnight under an argon atmosphere. The reaction mixture was then filtered, and the filtrate was evaporated to dryness. The crude product was purified by silica gel column chromatography using $CH_3CN/KNO_3.H_2O$ (12/1, v/v) as eluant. The fractions containing the target product were collected, and the solvent was evaporated. The resulting solid was dissolved in CH_3CN to remove the excess KNO_3 by filtration. After evaporation, the product $[Ru(bpy)_2(phen\text{-}DPA)](NO_3)_2$ was dissolved in a small amount (~5 mL) of deionized distilled water, and a saturated aqueous solution of NH_4PF_6 was added to give a red precipitate. The precipitate was filtered, washed with water, and dried. Complex **1** was obtained as a red solid (153 mg, 52% yield). ^1H NMR (400 MHz, CD_3CN): δ (ppm) = 8.42-8.61 (m, 6H), 8.28 (s, 1H), 8.09-8.13 (m, 4H), 7.99-8.02 (m, 2H), 7.74-7.85 (m, 4H), 7.58 (d, *J* = 7.2Hz,1H), 7.44-7.47 (m, 3H), 7.21-7.24 (m, 2H) 2.19-3.5 (m, 24H), 1.47 (s, 27 H). ESI-MS. Calcd. for $[M\text{-}PF_6^-]^+$: m/z 1308.45. Found: m/z 1308.45. Calcd. for $[M\text{-}2PF_6^-]^{2+}$: m/z 581.74. Found: m/z 581.74.

2.3 Synthesis of complex 2

A mixture of complex **1** (200 mg, 0.14 mmol), 6 mL of trifluoroacetic acid and 3 mL dichloromethane was stirred overnight at room temperature under an argon atmosphere. After evaporation, the residue was added into 30 mL of anhydrous Et_2O, and the mixture was refluxed with stirring for 1 h to remove the short chain impurities. The red solid was collected by filtration. After drying, complex **2** was obtained as a red solid (166 mg, 94% yield). ^1H NMR (400 MHz, CD_3CN): δ (ppm) = 8.51-8.53 (m, 1H), 8.34-8.39 (m, 5H), 8.19 (s, 1H), 7.76-8.04 (m, 8H), 7.44-7.57 (m, 4H), 7.23 (s, 2H), 7.02 (s, 2H), 2.82-3.84 (m, 24H), ^{13}C NMR (100 MHz, CD_3CN): δ (ppm) =

165.58, 165.29, 159.79, 159.58, 154.85, 154.35, 154.18, 153.96, 150.58, 148.79, 140.11, 140.01, 138.98, 134.91, 132.70, 129.86, 129.55, 129.43, 128.30, 127.96, 126.46, 125.30, 125.25, 119.98, 117.65, 68.52, 57.67, 49.18, 16.60, 10.73. ESI-MS. Calcd. for $[M\text{-}2PF_6^-]^{2+}$: m/z 497.65. Found: m/z 497.65. Elemental analysis (%) calcd for $C_{48}H_{51}N_{11}F_{12}O_7P_2Ru{\cdot}2CF_3COOH{\cdot}6H_2O$: C 38.53, H 4.04, N 9.50; found: C 38.39, H 4.15, N 9.52.

2.4 Synthesis of Ru-Gd

A mixture of complex **2** (50 mg, 0.04 mmol) and $GdCl_3{\cdot}6H_2O$ (19 mg, 0.05 mmol) in H_2O (3.0 mL) was stirred at room temperature for 24 h. After the pH value of the solution was adjusted to about 6.5 with 0.05 M NaOH, the solution was poured into 200 mL saturated aqueous solution of potassium nitrate, and stirred for 12 h. After lyophilized, the residue was dissolved in acetonitrile (50 mL) to remove the excess inorganic salts. The filtrate was evaporated to dryness to give **Ru-Gd** as a red solid (21 mg, 43% yield). ESI-MS. Calcd. for $[M\text{-}2NO_3^-]^{2+}$: m/z 575.15. Found: m/z (m/z): 575.15.

2.5 Syntheses of Ru-Eu and Ru-Tb

The complexes **Ru-Eu** and **Ru-Tb** were synthesized using the same method as described above by using $EuCl_3{\cdot}6H_2O$ and $TbCl_3{\cdot}6H_2O$ instead of $GdCl_3{\cdot}6H_2O$. **Ru-Eu**: ESI-MS. Calcd. for $[M\text{-}2NO_3^-]^{2+}$: m/z 572.60. Found: m/z: 572.54. **Ru-Tb**: ESI-MS. Calcd. for $[M\text{-}2NO_3^-]^{2+}$: m/z 575.60. Found: m/z: 575.60.

2.6 Luminescence imaging of live cells

HepG2 cells were cultured in RPMI-1640 medium (Sigma-Aldrich), supplemented with 10% fetal bovine serum (Corning Incorporated), 1% penicillin (Gibco), and 1% streptomycin (Gibco) at 37 °C in a 5% CO_2/95% air incubator. The cultured HepG2 cells in a glass bottom cell culture dish (ϕ=20 mm) were washed with PBS buffer, and then incubated in the PBS buffer containing 10 μM **Ru-Gd** and 0.01 μM dextran sulfate. After incubation for 15 min at 37 °C, the cells were washed three times with PBS buffer, and then subjected to the luminescence imaging measurements.

2.7 MTT assay

HepG2 cells were incubated (1×10^4 cells/mL) with different concentrations of **Ru-Gd** in fresh RPMI-1640 culture medium (containing 0.01 μM dextran sulfate) in 96-well cell culture plates at 37 °C in a 5% CO_2/95% air incubator for 4 h, and then the culture medium was removed. The cells were further incubated in the PBS buffer containing 250 μg/mL of MTT for an additional 4 h. The supernatants were removed, and the cell layer was dissolved in DMSO (100 μL). The absorbance at 540 nm of each well referenced at 620 nm was measured in a 96-well multi well-plate reader (Bio-Rad iMark).[32,33]

2.8 Luminescence imaging of *Daphnia magna*

Daphnia magna were raised in nonchlorinated tap water at 20 °C under a cool-white fluorescent light with a 14:10 h light:dark photoperiod. The culture medium was renewed three times a week. Scenedesmus obliquus were fed to Daphnia magna daily. The newborn Daphnia magna (age < 48 h) were incubated with **Ru-Gd** (100 μM) in the culture medium for 3 h at 25 °C, washed four times with culture medium, and then subjected to the luminescence imaging measurements.

2.9 Magnetic resonance properties of Ru-Gd

The longitudinal and transverse relaxation times of water solutions containing different concentrations of **Ru-Gd** were measured on 0.5 T NM12 magnetic resonance analyzer. The T_1-weighted MRI of water solutions containing different concentrations of **Ru-Gd** or Gadopentetate dimeglumine were carried out on 0.5 T NMI 20-030H-I magnetic resonance imager from NIUMAG technology. The longitudinal (r_1) and transverse (r_2) water proton relaxivities were estimated from the slopes in the plots of $1/T_1$ and $1/T_2$ versus the Gd^{3+} concentration, respectively.

2.10 MRI of KM mouse

The T_1-weighted MRI of KM mouse was carried out on 0.5 T NMI20-030H-I magnetic resonance imager from NIUMAG technology. A female KM mouse (purchased from Dalian Medical University) with a weight of ~20 g was used for the MRI measurements. The authors state that all animal studies were carried out at Specific Pathogen Free Animal Center at the Dalian Medical University according to the animal protocols (No. L2014014) approved by the Animal Ethics Committee (AEC). The mouse was anesthetized by 1.5% isoflurane in oxygen. The measurements were performed before and after intraperitoneal injection of **Ru-Gd** solution. The injection dose was 200 μL of the aqueous **Ru-Gd** solution (2 mM). After the measurements, the mouse was revived from anesthesia, placed into a cage, and given a free access to both food and water.

3. Results and discussion

3.1 Preparation of the Ru-Ln complexes

Luminescent Ru(II) complexes possess rich photochemical and photophysical properties, and high emission sensitivity in responding to changes of local environments,[34-37] which enable them to be modified for the design of various responsive luminescent imaging agents. Scheme 1 outlines the preparative strategies employed in this work to access the

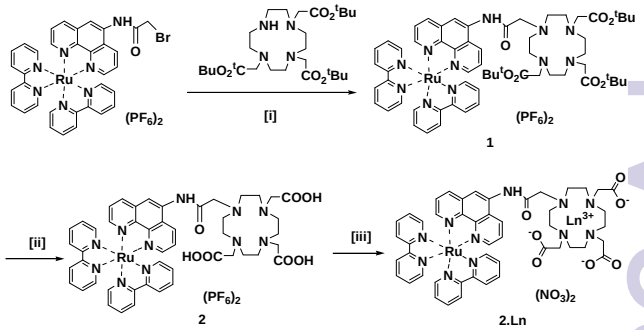

Scheme 1. Synthesis of heterobimetallic Ru(II)–Ln(III) complexes. [i] CH_3CN, reflux, overnight; [ii] CF_3CO_2H/CH_2Cl_2 (2:1), rt, overnight; [iii] $LnCl_3.6H_2O$, water (pH 6.5).

complex **2.Ln**. Alkylation of the well-known DO3A *tert*-butyl ester with $[Ru(bpy)_2(phen\text{-}Br)](PF_6)_2$ in the presence of cesium carbonate gave the complex **1**. Cleavage of the tert-butyl esters of complex **1** with trifluoroacetic acid gave the complex **2** in good yield. The composition of complex **2** was well confirmed by NMR spectroscopy, MS, and elementary analyses. Upon addition of Gd^{3+}, the complex $[Ru(bpy)_2(phen\text{-}DOTA\text{-}Gd)](NO_3)_2$ (**Ru-Gd**) was obtained, which was confirmed by mass spectrum with a signal at *m/z* 574.13 ($[M\text{-}2NO_3^-]^{2+}$). Moreover, we also focused on the use of d-block metal complexes as sensitizers for lanthanide luminescence, so **Ru-Eu** and **Ru-Tb** were synthesized according the above method, respectively.

3.2 UV-vis absorption and photophysical properties of the Ru-Ln complexes

The UV-vis absorption and photophysical properties of the heterobimetallic Ru(II)–Ln(III) complexes were measured in PBS buffer (50 mM, pH=7.4). As shown in Fig. 1, complex **2**, **Ru-Gd, Ru-Eu** and **Ru-Tb** exhibited the same absorption pattern with absorption peaks centred at ~290 nm and ~450 nm, assigned to the spin-allowed ligand localized $\pi \rightarrow \pi^*$ transition and metal-to-ligand charge transfer (MLCT) transition of the Ru(II) complex, respectively. Fig. S10 showed the excitation and emission spectra of the **Ru-Ln** complexes. Under the excitation of 450 nm light, all the complexes emitted the strongly red phosphorescence at 605 nm, and the emission intensity and pattern of the Ru(II) complex were not influenced by intramolecular adjacent Eu(III), Tb(III) and Gd(III) ions. These results indicate that the energy transfer between the Ru(II) complex and lanthanide ions does not occur, and the Ru(II) complex-based chromophore cannot sensitize the emission of Eu(III) and Tb(III) ions. In addition, the measurement of transient luminous efficiency exhibited that the luminescence lifetime of **Ru-Gd** reached to 688 ns at room temperature, which is much longer than those of organic dyes and ideal for generating high-resolution luminescence images.

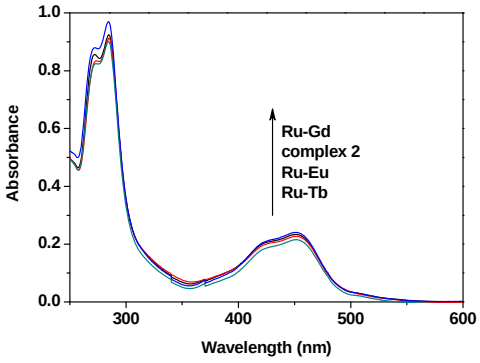

Fig. 1. UV-vis absorption spectra of complex 2, Ru-Eu, Ru-Tb, and Ru-Gd.

3.3 Luminescent imaging application of Ru-Gd for live cells

At first, the cytotoxicity of **Ru-Gd** to live cells and its stability in the cellular environment were investigated. In the test, human liver carcinoma cells (HepG2) were incubated with different concentration of **Ru-Gd**, and then the cell proliferation and viability were analyzed by the MTT assay. As shown in Fig. 2D, the cell viabilities were still greater than 90% even the cells were incubated with high concentrations of **Ru-Gd** (<100 μM), which indicates that **Ru-Gd** is low-cytotoxic, and stable in the cellular environment without noticeable degradation and metal ion release. Next, the applicability of **Ru-Gd** for the luminescent imaging of live cells was investigated. HepG2 cells were incubated with **Ru-Gd** (10 μM) in a 5% CO_2/95% air incubator in 10 mM PBS buffer of pH 7.4. After incubation for 15 min at 37 °C, clearly red intracellular luminescence was observed both in the nuclear region and cytoplasm (Fig. 2B). This result demonstrates that the novel magnetoluminescent imaging agent, **Ru-Gd,** can truly be used for the luminescence imaging of live cancer cells.

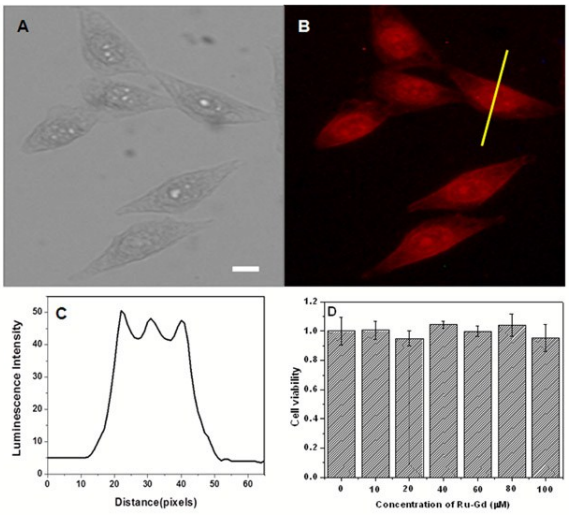

Fig. 2. Luminescence images of HepG2 cells incubated with **Ru-Gd** (10 μM). A: bright field image (scale bar: 5 μm); B: luminescence image (excitation filter, 450-490 nm; dichroic mirror, 505 nm; emission filter, > 590 nm); C luminescence intensity profiles of **Ru-Gd** in the interest linear region across a HepG2 cell (yellow line in B); D: viabilities of the HepG2 cells after incubated with different concentrations of **Ru-Gd.** Image analysis was performed using Image J software.

3.4 Luminescent imaging application of Ru-Gd for Daphnia magna

After the cell imaging investigation，we estimated the utility of **Ru-Gd** for luminescence imaging in living *Daphnia magna,* a widely used laboratory animal as an indicator of aquatic ecosystem health and as a model animal in ecotoxicology.[38] As

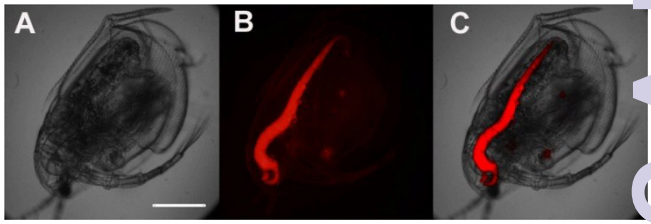

Fig. 3. In vivo Luminescence images of Daphnia magna incubated with **Ru-Gd** (100 μM) for 3 hours. A: bright field image; B: luminescence image (excitation filter, 450-490 nm; dichroic mirror, 505 nm; emission filter, > 590 nm); C: merged image of A and B. scale bar: 700 μm.

shown in Fig. 3, after incubated with **Ru-Gd**, *Daphnia magna* showed strongly red luminescence signals mainly in the range of esophagus, midgut and hindgut, which revealed that the probe molecules were transferred into the body of *Daphnia magna* through their food process. The result demonstrates that the novel magnetoluminescent imaging agent, **Ru-Gd,** is a useful tool for the luminescence imaging in vivo.

3.5 Magnetic resonance properties of Ru-Gd

The ability of magnetoluminescent imaging agent **Ru-Gd** to shorten the longitudinal relaxation time (T_1) and transverse relaxation time (T_2) is expressed in terms of longitudinal (r_1) and transverse (r_2) relaxativity, respectively ($r_{1,2}=((1/T_{1,2})_{observed}-(1/T_{1,2})_{diamagnetic})/[Gd(III)]$).[39] To determine r_1 and r_2 of **Ru-Gd**, the concentration-dependent measurements of the relaxation times were performed in H_2O (Fig. 4), giving a r_1 of 4.71 mM^{-1} s^{-1} and a r_2 of 5.69 mM^{-1} s^{-1}, respectively. The r_2/r_1 ratio was calculated to be 1.2, indicating that **Ru-Gd** should be a T_1 contrast agent. The longitudinal relaxivity of **Ru-Gd** is relatively higher than that of the parent Gd-DOTA complex (3.5-4.2 mM^{-1} s^{-1}), which presumably is due to the slower molecular tumbling of the gadolinium complex as a result of the higher molecular weight. Furthermore, the comparable r_1 suggested that at least one inner-sphere water molecule was bound to the lanthanide ion center.[39] As shown in Fig. 4, a T_1-weighted image (TR=300; TE=19) of distilled water and serial dilutions of **Ru-Gd** (containing 0.025, 0.2, 0.4 and 0.6 mM of **Ru-Gd**) were acquired with a commercial 0.5 T magnetic resonance analyzer, and the signal intensity in T_1-weighted images showed an obvious dose-dependent enhancement. For evaluating the applicability of **Ru-Gd** as T_1 contrast agent, the Gadopentetate dimeglumine**,** a widely used T_1 contrast agent in clinic, was used as a control agent for T_1-weighted MR image in the same condition. As shown in Fig. 4, the signal intensity of **Ru-Gd** and Gadopentetate

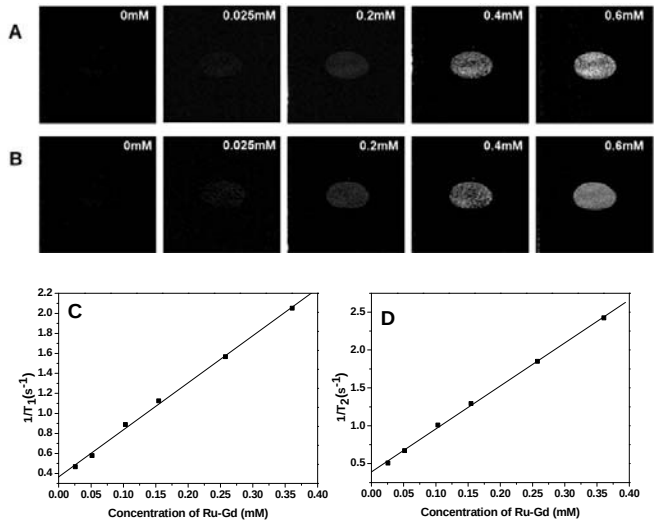

Fig. 4. T_1-weighted MR images of water solutions containing different concentrations of **Ru-Gd** (A); Gadopentetate dimeglumine (B), and fitted curves of relaxation rates of **Ru-Gd** in water (C and D). B: T_1 mode; C: T_2 mode; Y-axis: reciprocal of the relaxation time; X-axis: concentration of **Ru-Gd** (0.0025, 0.05, 0.1, 0.15, 0.25, and 0.35 mM).

dimeglumineare almost the same under the same conditions due to the close r_1 (4.95 mM^{-1} s^{-1} for Gadopentetat dimeglumine and 4.71 mM^{-1} s^{-1} for **Ru-Gd**). These results demonstrated the ability of **Ru-Gd** to act as an effective T_1 contrast agent at lower micromolar concentration level.

3.6 MRI application of Ru-Gd for live organisms

Since MRI contrast agents were eventually used in living bodies, a further exploratory effort was made to evaluate the applicability of **Ru-Gd** for the T_1-weighted MRI of living KM mouse, a widely used laboratory animal in MRI experiments. In the experiment, a female isoflurane-anesthetized KM mouse (weight 20 g) was taken **Ru-Gd** (0.2 ml, 2 mM) by intraperitoneal injection to investigate the feasibility of **Ru-Gd** for the in vivo MRI. After injection, the **Ru-Gd**-loaded KM mouse was subjected to a commercial 0.5T Animal MRI System for monitoring the distribution and metabolism of **Ru-Gd** wi T_1-weighted MRI method. Fig. 5 shows the T_1-weighted M transection images of the interest portions of **Ru-Gd**-loaded KM mouse at multiple time points after injection, and Fig. S1 shows the T_1-weighted MR sagittalsection images of the same mouse at the same time points. As shown in Fig. 5 and Fig. S11, a clearly bright contrast enhancement was observed in the post-injection mouse bladder after 5 min. The bright contra enhancement in mouse bladder maintained up to 6 h after injection, and then gradually returned to almost zero after 22 h due likely to the excretion of **Ru-Gd**. These results reveal that the magnetoluminescent imaging agent **Ru-Gd** has a long retention time in living bodies, which could be benefit to track MR signals over a long time scale. Furthermore, the KM mouse was still healthy survival after the test, which suggests that **Ru-Gd** is biocompatible with low-toxic, and could be a useful contrast agent for the T_1-weighted *in vivo* MRI application.

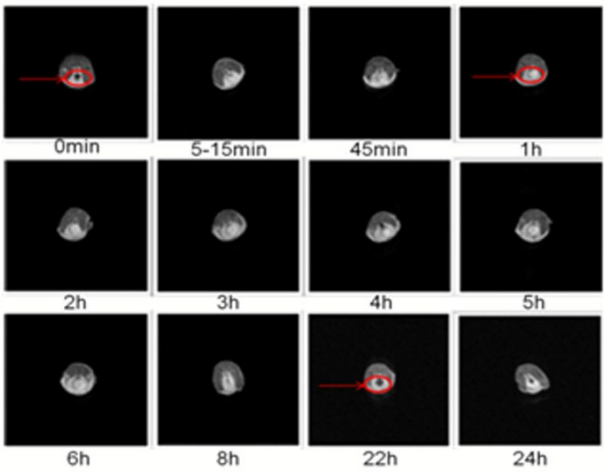

Fig. 5. T1-weighted MR transection images of KM mouse, which show abdominal cavity cross section at different monitoring times (0 min, 5 min, 15 min, 45 min, 1 h, 2 h, 3 h, 4 h, 5 h, 6 h, 8 h, 22 h, 24 h) after intraperitoneal injection of Ru-Gd (2 mM, 0.2 mL). The red circles indicate the bladder of the mouse.

4. Conclusions

In summary, we have designed and synthesized a novel magnetoluminescent dual-modal imaging agent, **Ru-Gd,** by coupling a Ru(II) complex with a Gd(III) complex. The complex **Ru-Gd** possesses several advantageous properties, such as excellent solubility in water, good biocompatibility, visible-light absorption and emission, large Stokes shift, high photochemical stability, and long luminescence lifetime, which enables the complex to be favorably useful for the luminescent imaging of living cells. In addition, the evaluation of the data collected from the water relaxation experiments indicates that **Ru-Gd** is an active agent for the T_1-wighted MRI. The results of luminescent imaging for living cells and in vivo MRI for Kunming mouse demonstrated the practical applicability of **Ru-Gd** as an efficient dual-modal imaging agent. Further studies on the attachment of a functional luminescent Ru(II) complex to a Gd^{3+} complex-based contrast agent will lead the magnetoluminescent imaging agent to track interested biological targets such as cancer cells in vitro and in vivo.

Acknowledgements

Financial support from the National Natural Science Foundation of China (Grant No. 21475016), the Specialized Research Fund for the Doctoral Program of Higher Education of China (Grant No. 20130041120024) and the Fundamental Research Funds for the Central Universities (DUT15ZD116, DUT15TD14) is gratefully acknowledged.

Notes and references

1 R.Weissleder and M. J. Pittet, *Nature.,* 2008, **452**, 580−589.
2 H. Kobayashi, M.Ogawa, R.Alford, P. L.Choyke, Y.Urano and *Chem. Rev.,* 2010, **110,** 2620−2640.
3 J. Xie and X. Chen, *Biomedical Imaging: The Chemistry of Labels, Probes and Contrast Agents*., 2012, 465-489.
4 M. H. Keefe, K. D. Benkstein and J. T. Hupp, *Coord. Chem. Rev.,* 2000, **205,** 201–228.
5 A. Hellebust and R. R. Kortum, *Nanomedicine (London, United Kingdom)*, 2012, **7**, 429-445.
6 A. Beeby, S. W. Botchway, I. M. Clarkson, S. Faulkner, A. W. Parker, D. Parker and J. A. G. Williams, *J. Photochem. Photobiol. B: Biology,* 2000, **57**, 83-89.
7 L. J. Charbonnie`re, R. Ziessel, M. Montalti, L. Prodi, N. Zaccheroni, C. Boehme and G. Wipff, *J. Am. Chem. Soc.,* 2002, **124**, 7779-7788.
8 S. Aime, A.Barge, C.Cabella, S. G. Crich and E. Gianolio, *Curr. Pharm. Biotechnol.,* 2004, **5,** 509-518.
9 M. Bottrill, L. Kwok and N. J. Long, *Chem. Soc. Rev.,* 2006, **35**, 557-571.
10 A. Francois, C. Auzanneau,V. L. Morvan,C. Galaup, H. S. Godfrey, L. Marty,A. Boulay, M. Artigau, B. M. Voegtle, N. Leygue, C. picard, Y. Coulais, J. Robert and E. Benoist, *Dalton Trans.*, 2014, **43,** 439–450.
11 L. E. Jennings and N. J. Long, *Chem. Commun.,* 2009, 3511–3524.
12 W. Xu, B. A. Bony, C. R. Kim, J. S. Baeck, Y. Chang, J. E. Bae, K. S. Chae, T. J. Kim and G. H. Lee, *Sci. Rep.,* 2013, **3,** 3210-3219.
13 X. He, K. Wang and Z. Cheng, *Wiley Interdiscip. Rev.: Nanomed. Nanobiotechnol.,* 2010, **2,** 349−366.
14 P. Caravan, *Chem. Soc. Rev.,* 2006, **35,** 512-523.
15 F. Erogbogbo, C. W. Chang, J. May, L. Liu, R. Kumar, W. Law, H. Ding, K. Yong, I. Roy, M. Sheshadri, M. Swihart and P. Prasad, *Nanoscale*, 2012, **4**, 5483-5489.
16 H. B. Na and T. Hyeon, *J. Mater. Chem.,* 2009,**19**, 6267-6273
17 E. Toth, L. Helm and A. E. Merbach, *Top. Curr. Chem.,* 2002, **221,** 61-101.
18 P. Pyykko, *Nat. Chem.,* 2015, **7,** 680-689.
19 S. Aime, S. G. Crich, E.Gianolio, G. B. Giovenzana, L. Tei and E. Terreno, *Coord. Chem. Rev.,* 2006, **250**, 1562-1579.
20 M. W. Ahmad, W. Xu, S. Kim, J. Baeck, Y. Chang, J. Bae, K. Chae,; J. Park, T. Kim and G. Lee, *Sci. Rep.,* 2015, **5**, 8549-8560.
21 A. Louie, Chem. Rev., 2010, **110 (5)**, 3146–3195.
22 Y. Xiao, Y. Wu, W. Zhang, X. Li and F. Pei, *Chin. J. Anal. Chem.,* 2011, **5**, 757-764.
23 A. Mishra, J. Pfeuffer, R. Mishra, J. Engelmann, A.Mishra, K. Ugurbil and N. Logothetis, *Bioconjugate Chem.,* 2006, **17 (3)**, 773–780.
24 M. M.Hüber, A. B. Staubli, K. Kustedjo, M. H. B. Gray, J. Shih, S. E. Fraser, R. E. Jacobs and T. J. Meade, *Bioconjug Chem.,*1998, **9 (2)**, 242–249.
25 H. Li, B. D.Gray, I. Corbin,C. Lebherz, H. Choi, S. Lund-Katz, M. Wilson, J. D. Glickson and R. Zhou, *Academic Radiology*, 2004, **11,** 1251-1259.
26 Q. Zhao, C. Huang and F. Li, *Chem. Soc. Rev.,* 2011, **40,** 2508-2524.
27 G. Dehaen, P. Verwilst, S. V. Eliseeva, S. Laurent, L. V. Elst, R N. Muller, W. M. D. Borggraeve, K. Binnemans and T. N. Parac-Vogt, *Inorg. Chem.,* 2011, **50,** 10005-10014.
28 K. Thelma and S. Louise, *J. Am. Chem. Soc.,* 2008, **130,** 2178-2179.
29 R. Zhang, Z. Ye, Y. Yin, G. Wang, D. Jin, J. Yuan and J. A. Piper, *Bioconjugate Chem.,* 2012, **23 (4)**, 725–733.
30 A. Dadabhoy, S. Faulkner and P. G. Sammes, *J. Chem. Soc. Perkin Trans.,* 2002, 348-357.
31 S. Mizukami, K. Tonai, M. Kaneko and K. Kikuchi, *J. Am. Chem. Soc.,* 2008, **130,** 14376-14377.
32 O. Zava, S. M. Zakeeruddin, C. Danelon, H. Vogel, M. Grätzel, and P. J. Dyson, *ChemBioChem.,* 2009, **10,** 1796-1800
33 U. Schatzschneider, J. Niesel, I. Ott, R. Gust, H. Alborzinia and S. Wölfl, *ChemMedChem.,* 2008, **3,** 1104-1109.
34 E. C. Glazer, D. Magde and Y. Tor, *J. Am. Chem. Soc.,* 2007, **129,** 8544−8551.
35 N. H. Damrauer, T. R.Boussie, M. Devenney and J. K. McCusker, *J. Am. Chem. Soc.,* 1997, **119**, 8253−8268.
36 Z. Ye, R. Zhang, B. Song, Z. Dai, D. Jin, E. M.Goldys and J. Yuan, *Dalton Trans.,* 2014, **43,** 8414-8420.
37 R. Zhang, Z. Ye, Y. Yin, G. Wang, D. Jin, J. Yuan and J. A. Piper, *Bioconjugate Chem.,* 2012, **23 (4)**, 725–733.
38 S. B. Lovern and R. Klaper, *Environ. Toxicol.Chem.,* 2006, **25,** 1132-1137.
39 P. Caravan, J. J. Ellison, T. J. McMurry and R. B. Lauffer, *Chem Rev.,*1999, **99,** 2293−2352.

Table of contents:

A novel heterobimetallic ruthenium(II)-Gadolinium(III) complex, **Ru-Gd,** has been developed for luminescence and in vivo T_1-weighted MR imaging agent.